



Renewable hydrogen production by a mild-temperature steam reforming of the model compound acetic acid derived from bio-oil

Zhikun Li^{a,b}, Xun Hu^{a,c}, Lijun Zhang^c, Gongxuan Lu^{a,*}

^a State Key Laboratory for Oxo Synthesis and Selective Oxidation, Lanzhou Institute of Chemical Physics, Chinese Academy of Sciences, Lanzhou 730000, PR China

^b The Graduate School of Chinese Academy of Sciences, Beijing 100039, PR China

^c Curtin University of Technology, Perth, WA 6845, Australia

ARTICLE INFO

Article history:

Received 4 October 2011

Received in revised form 5 December 2011

Accepted 6 December 2011

Available online 15 December 2011

Keywords:

Acetic acid

Hydrogen

Steam reforming

Ni/La₂O₃

ABSTRACT

In this study, steam reforming of acetic acid over Ni/La₂O₃ catalyst for hydrogen generation was investigated. The experiments were carried out by varying the reaction conditions such as Ni content, reaction temperature, liquid hourly space velocity (LHSV) and steam-to-carbon ratios (S/C), to evaluate the influences of these parameters on the steam reforming reactions for getting the best catalytic performances. The results showed that the Ni/La₂O₃ catalyst with the Ni loading of 20 wt.% presented the superior activity and selectivity. The reaction temperature, LHSV and S/C strongly influenced the reforming reactions. At $T = 623$ K, $LHSV = 5.1 \text{ h}^{-1}$ and $S/C = 7.5:1$, the catalyst exhibited the best performances, acetic acid was converted completely, and selectivity to hydrogen exceeded 93%. Moreover, the catalyst presented rather stable performances for the 100 h time-on-stream without any deactivation. Besides, the reaction pathways were also discussed, methyl species was the important intermediate in the reforming reactions, which was the precursors for the formation of the gaseous products, while hydroxyl species was another important intermediate that was important for the formation of hydrogen and elimination of the by-products.

© 2011 Elsevier B.V. All rights reserved.

1. Introduction

Hydrogen, as the cleanest fuel and energy carrier, is not only widely used for chemical and petrochemical industry, but also is the important fuel for the high efficiency fuel cells [1]. Presently, hydrogen is produced commercially, mostly from natural gas, liquefied petroleum gas, and naphtha, by catalytic steam reforming or partial oxidation of heavy oil fractions [2,3]. However, now it is necessary to produce hydrogen from an alternative energy source, owing to the concerns about the depletion of fossil fuel reserves and the pollution caused by continuously increasing energy demands. Biomass is not only a resource of renewable and environmentally preferable energy, but also can achieve the zero emission of carbon dioxide in the hydrogen production cycle, for the fact that the carbon dioxide released into the atmosphere is offset by the uptake of carbon dioxide during biomass growth. Thus, biomass can be a sustainable and renewable source for the production of chemicals including hydrogen [4,5]. The hydrogen from biomass can be obtained using several methods, including pyrolysis, gasification and steam reforming [6]. Of special interest are methods in which biomass is converted to intermediate liquid bio-oil and

its subsequent steam reforming, for bio-oil has the advantages of high energy density and ease of handling, and most importantly, it is the fact that it can be used directly for the on-demand hydrogen production for fuel cells. However, bio-oil is a complex mixture of oxygenate compounds, and design of an effective catalyst for bio-oil steam reforming require to investigate a model oxygenate firstly to obtain the fundamental knowledge of steam reforming the complicated mixture of the organic molecules. Acetic acid is one of the major components in bio-oil [7,8], therefore, study of steam reforming of acetic acid can provide valuable methods and data for hydrogen production from bio-oil. In addition, acetic acid itself is renewable, which can be easily obtained from biomass by fermentation. And acetic acid, unlike methanol and ethanol, is noninflammable, hence, it is a safe hydrogen carrier. Moreover, acetic acid also can be easily converted to hydrogen with high selectivity at relatively low reaction temperature over effective catalysts; hence, it also may be one of the suitable fuels for the proton exchange membrane fuel cells (PEMFC).

Up to now, although much work has been carried out on steam reforming of methanol and ethanol, only a few papers appeared in the open literature dealt with the conversion of acetic acid to hydrogen [8–16]. And the catalysts investigated are limited to ICI 46-1 [8,9], UC G-90C [8–10], Ni–Al [11,12], Pt/ZrO₂ [13–15], Pt, Rh and Pd based catalysts [16]. Usually, the temperature conducted in the reforming reactions over these catalysts was higher than

* Corresponding author. Tel.: +86 931 4968178; fax: +86 931 4968178.

E-mail address: gxlu@lzb.ac.cn (G. Lu).

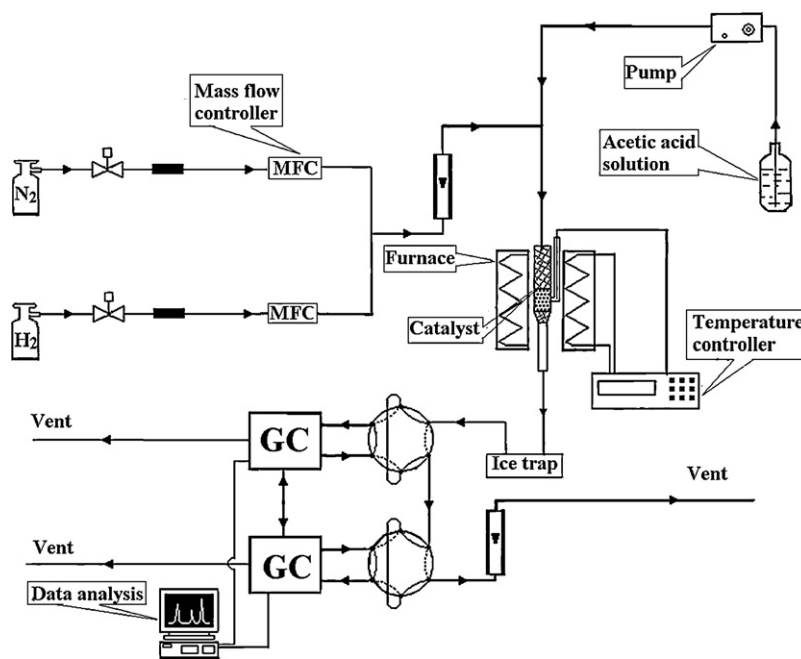


Fig. 1. Schematic diagram of the reactor system for steam reforming of acetic acid.

873 K, and there were always appreciable amounts of organic and gaseous by-products generation, which resulted in the low selectivity to hydrogen. Therefore, an issue of major importance is then to develop a catalyst exhibiting high activity and stability with high hydrogen yields at relatively lower reaction temperature.

In our previous work [17,18], we have reported Fe–Co and Ni–Co catalysts for acetic acid reforming, which showed good activity and selectivity to hydrogen, complete conversion of acetic acid could be achieved at 673 K. While in this paper, a novel supported catalyst Ni/La₂O₃ for steam reforming of acetic acid was presented, which was chosen based on the following consideration. Among transition metals, Ni was reported as the efficient material for the C–C bond cleavage [19] and showed good activity for hydrogenation [20], dehydrogenation [21] reactions, more importantly, it has been widely investigated for methanol decomposition [22] and ethanol reforming [23,24] reactions because of its high activity and low cost. Therefore, in this paper Ni was selected as the active metal for acetic acid reforming. Besides, the nature of the support also plays a key role in determining the catalytic performance since it affects dispersion and stability of the metal as well as it may participate in the reaction, hence choice of the support is crucial. Lanthanum oxide was recognized as a good support for metals that catalyze reactions such as methanol decomposition [25], ammonia oxidation [26], and methane dry reforming [27]. Moreover, it has also shown that lanthanum oxides can substantially modify the chemical behavior of highly dispersed metal catalysts [28], and it contained medium and strong basic sites [29], which could favor water adsorption and OH surface mobility and then aid the steam reforming [30,31]. Thus, La₂O₃ was selected as the support. In addition, Ni/La₂O₃ catalyst has been previously investigated for the steam reforming of ethanol and exhibited excellent activity and selectivity [32–34]. Based on the reasons mentioned above, the Ni/La₂O₃ catalyst was chosen and investigated in detail for the steam reforming acetic acid in this paper.

The study was carried out by varying the operating reaction conditions, such as Ni loadings, reaction temperature, steam to carbon ratios, space velocity and so on, with the aim of getting the maximum catalytic activity and hydrogen yields. The catalyst was characterized by temperature-programmed reduction

technique (TPR), X-ray photoelectron spectroscopy (XPS) and BET method, respectively. The reaction pathways of steam reforming of acetic acid were also discussed. The results showed that under the selected experimental conditions, acetic acid could be converted completely at the temperature as low as 623 K, with the selectivity toward hydrogen exceeded 93%, to our knowledge, such results have not been reported at such low reaction temperature.

2. Experimental

2.1. Catalyst preparation

Ni/La₂O₃ catalysts were prepared by the method of incipient wetness impregnation using nickel nitrate as a metal precursor. The amount of Ni loadings on the catalyst was controlled at 0–26 wt.% by varying the concentration of Ni(NO₃)₂ solution. Before impregnation, La₂O₃ support was stabilized in air at 873 K for 3 h, surface area of the treated sample was 10.67 m² g⁻¹. After impregnation, the catalysts precursors were dried at room temperature for 24 h, subsequently dried at 383 K for another 24 h and finally calcined at 773 K for 4 h. The catalyst powder was tabletted and then crushed into particles with 0.20–0.56 mm size for use.

2.2. Catalytic activity measurements

The experimental reactor system, consisting of a flow controller unit, the reactor unit and the analysis unit, was constructed as showed in Fig. 1. Catalytic performances tests were carried out in a fixed bed continuous flow quartz reactor (i.d. 8 mm) at atmospheric pressure and temperature from 523 to 873 K. Typically, 0.8 g of catalyst was used in each run and diluted with equal amount of quartz. Prior to each experiment, the calcined catalyst was reduced in situ at $T=673$ K, for 3 h, under a 50% H₂ in N₂ stream (flow rate 60 mL/min). The feed was then switched to N₂ and the reactor was equilibrated at the desired reaction temperature, the pre-mixed acetic acid solution with a certain steam to carbon ratio was then fed to the reactor by a syringe at a varied flow rate, which depended on the different runs of the experiment. N₂ was used as a carrier gas and internal standard for

gas analysis. The separation and quantification of the gas phase effluents were attained on two on-line chromatograms equipped with thermal-conductivity detectors (TCD). Hydrocarbons as well as oxygenated products were separated and analyzed by a flame ionization detector (FID). At the end of the catalytic tests, the flow of acetic acid solution was stopped and the catalysts were cooled under a N_2 stream and stored for further characterizations. Steam reforming activity was defined in terms of conversions of acetic acid and selectivities to the products. The conversions of acetic acid were denoted as C in the figures and tables. While the selectivities to the products (hydrogen, carbon dioxide, methane, carbon monoxide and so on) were denoted as S_{product} , which were calculated according to the corresponding equations: $S_{H_2} (\%) = 100 \times (\text{moles of } H_2 \text{ production}) / (\text{moles of acetic acid consumed} \times 4)$; the calculated method of other products' selectivities were similar to that of H_2 . Moreover, liquid hourly space velocity (LHSV) here was defined as (volumetric flow rate of feed solution ($\text{cm}^3 \text{ h}^{-1}$))/(catalyst bed volume (cm^3)). Another parameter used to indicate the proportion of acetic acid and steam was steam to carbon ratios (S/C), which was defined by the formula: $S/C = (\text{moles of steam in the feed}) / (\text{moles of carbon in the feed})$.

2.3. Catalyst characterization

The H_2 temperature-programmed reduction technique (TPR) experiments over the series calcined catalysts were carried out in a conventional flow system built in our laboratory. The curves were obtained by passing a 5% H_2 in Ar stream (flow rate: 40 mL/min) through the catalysts (10 mg). The temperature was increased from 298 to 1023 K at a linearly programmed rate of 20 K/min. The effluent gas was passed through a 13 \times molecular sieve to remove the steam from the exit stream and the amount of H_2 consumed was determined by a chromatogram.

The X-ray photoelectron spectroscopy (XPS) measurements were carried out at a room temperature on a VG ESCALAB 210 spectrometer with Mg $K\alpha$ radiation ($h\nu = 1253.6 \text{ eV}$). The binding energy was calibrated by the C_{1s} binding energy of 285.0 eV.

The specific surface area of the catalyst was measured by BET method on a Micromeritics ASAP-2010 apparatus at a liquid nitrogen temperature with N_2 as the absorbent at 77 K.

One point clarified here was that the XPS and BET characterizations were all conducted over the Ni/La_2O_3 catalyst with the Ni loadings of 20 wt.%, for it exhibited the superior activity among the series catalysts with different Ni contents, which would be discussed below in detail (see Section 3.3).

3. Results and discussion

3.1. Catalysts characterization

H_2 -TPR is a powerful tool to study the reduction behavior of the oxides phase, from which it is possible to obtain useful information about the degree of the interactions between the species. Results of H_2 -TPR analysis profiles for the different metal loadings of Ni/La_2O_3 catalysts were presented in Fig. 2. It could be found that no hydrogen consumption was observed for La_2O_3 , obviously, the support could not be reduced under the reduction conditions. While for the Ni-based catalysts, the amounts of hydrogen uptakes increased with the increase of Ni loadings and the uptakes are approximately in accordance with the catalyst compositions. However, although the catalysts exhibited comparable TPR profiles, the profiles still could be roughly divided into two types. For the catalysts with the Ni loading lower than 20 wt.%, the TPR profiles showed mainly one principle peak at ca. 700 K and two tail peaks at 930 and 1020 K, respectively. Evidently, there were three types Ni on La_2O_3 surface,

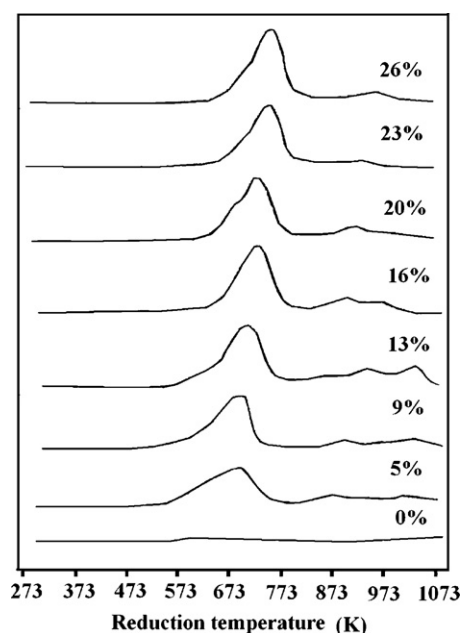


Fig. 2. H_2 TPR for the series of Ni/La_2O_3 catalysts.

the reduction temperature of which depended on the degrees of its interaction with the support. The low-temperature peak might be assigned to well-dispersed nickel oxide on the support while the two high-temperature peaks suggested that the reducibility of some of the nickel ions decreased by strong interactions with the support. While for the catalyst with the Ni loadings higher than 20 wt.%, there were two types of Ni on La_2O_3 surface. The profiles showed one shoulder at ca. 683 K and a principle peak at 733 K and a tail peak at about 910 K. The shoulder and the principle peak should be attributed to the reductions of the small and large particles of NiO , respectively. The appearance of the shoulder was probably caused by the slow hydrogen diffusion, suggesting an increase of the mean sizes of NiO particles with the increase of Ni loadings. The long tail peak in higher temperature region was corresponding to the second types Ni that had strong interactions with the support. Besides, we also conducted the H_2 TPR characterization over the pure NiO oxides that come from the calcination of $Ni(NO_3)_2$, the profiles showed one single peak at ca. 786 K. While the main reduction peak of NiO on La_2O_3 surface shifted to the lower temperature regions by almost 70 K, indicating the promotion effect of La_2O_3 . It had also been reported that La_2O_3 could promote the dispersion of nickel and further improve its reduction behaviors [35–37].

The XPS measurements were also conducted to get the catalyst surface information over the calcined, reduced and spent Ni/La_2O_3 catalysts, respectively. However, it could be seen from Fig. 3 that the binding energy of $Ni 2p_{3/2}$ in the reduced and spent catalysts were overlapped by that of $La 3d_{5/2}$, hence the binding energy was hard to be calculated. Similar results also were reported by Sun et al. [33]. While the binding energy of $Ni 2p_{3/2}$ at 854.87 eV in the calcined catalyst indicated that Ni species existed as NiO state, but there were positive shift of the binding energy when compared with the standard values, which might be influenced by the formation of $LaNiO_3$ species in the calcined process. For the Ni species in the reduced and spent catalysts, we speculated that it mainly existed as metal Ni on catalyst surface, according to the TPR results and the clear change of the spectroscopy of $Ni 2p$ shown in Fig. 3. Evidently, in the steam reforming process metal Ni was the active species. As for La species, the binding energy of $La 3d_{5/2}$ in the calcined catalyst was about 834.91 eV (Fig. 4), indicating that La species existed as La (III) species, however, in the reduced and spent catalyst the binding

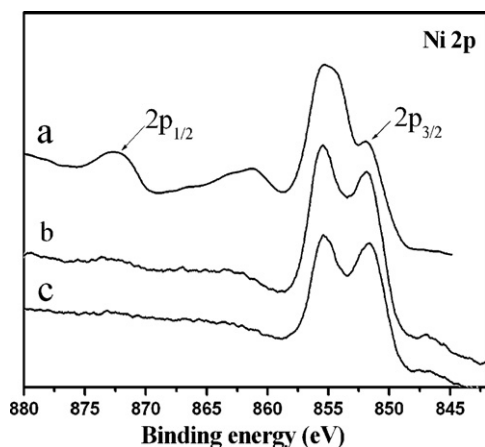


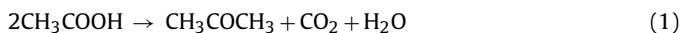
Fig. 3. XPS spectra of Ni 2p for the calcined, reduced and spent Ni/La₂O₃ catalysts (20 wt.%). (a) The calcined catalyst; (b) the reduced catalyst; (c) the spent catalyst.

energy of it shifted to about 835.30 eV, probably owing to the strong interactions between Ni and La species.

The results of BET measurements showed that the specific area of the Ni/La₂O₃ catalyst was relatively little, 11.27 m² g⁻¹, the total volume of pores and average pore diameter were 0.065 cm³ g⁻¹ and 17.86 nm, respectively.

3.2. Homogeneous (non-catalytic) reaction

In order to gain an idea of the homogeneous reactions of the reactants before them reaching the catalyst bed, the steam reforming of acetic acid was primarily investigated in the absence of catalyst. Results were shown in Fig. 5. It was observed that in the temperature range of 523–623 K the homogeneous reaction occurred just to a negligible extent. Only a trace amount of acetone detected in the effluent products indicated the bimolecular ketonization reaction of acetic acid [Eq. (1)] took place initially, whereas at 673 K, the acetic acid dehydration and decomposition proceeded [Eqs. (2) and (3)], resulting in the clear increase of ketene and methane amounts.



Furthermore, as temperature increase up to about 823 K, small quantities of CO were detected in the effluent gas, which might

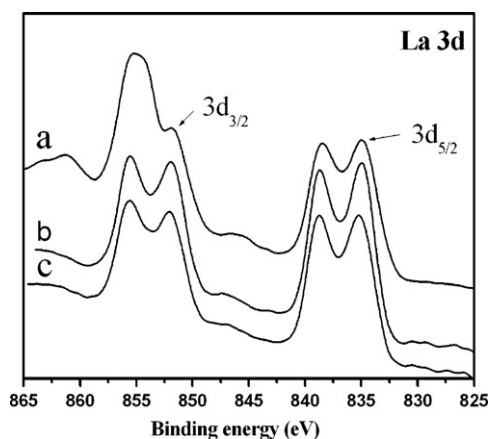


Fig. 4. XPS spectra of La 3d for the calcined, reduced and spent Ni/La₂O₃ catalysts (20 wt.%). (a) The calcined catalyst; (b) the reduced catalyst; (c) the spent catalyst.

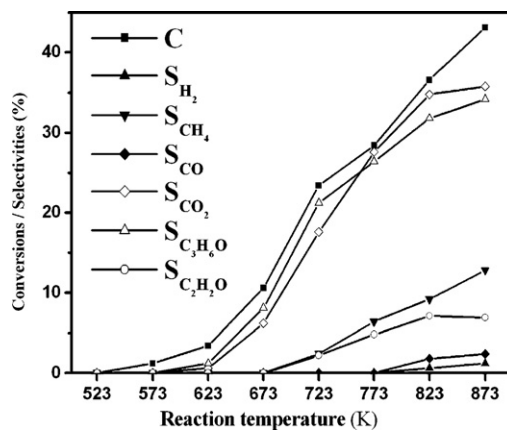


Fig. 5. The homogeneous reactions (in the absence catalyst), S/C ratio 7.5:1; LHSV = 5.1 h⁻¹; P = 1 atm.

come from the further decomposition of acetic acid. Besides, in the whole temperature range investigated there was almost no H₂ generation, suggesting that the steam reforming acetic acid [Eq. (4)] could not take place in the absence of catalyst.



3.3. Effects of Ni loadings

It is well established that catalyst composition has significant influences on catalyst behaviors, such as the activity and selectivity. Therefore, the Ni loadings were varied in the range of 0–26 wt.% to identify the optimal catalyst compositions for achieving the best catalytic performances. The series catalysts were evaluated from 523 to 873 K and results were shown in Fig. 6 and Table 1. It could be observed that the catalyst La₂O₃ without Ni loading showed very poor activity for acetic acid reforming. Acetic acid conversion could not attain 80% even at 873 K and only very small amount of H₂ was formed over the catalyst, in contrast, pronounced amount of acetone, ketene and CH₄ were produced, indicating that steam could hardly participate in the reactions, only the ketonization, dehydration and decomposition of acetic acid itself occurred. Although the La₂O₃ showed negligible activity toward the steam reforming, it showed some activity for the conversion of acetic acid via the dehydration and the ketonization reactions when compared with that of the blank test (the homogeneous reaction). While for the Ni-based catalysts, they all showed good activity for converting acetic acid, obviously, Ni was the active species that catalyzed the steam

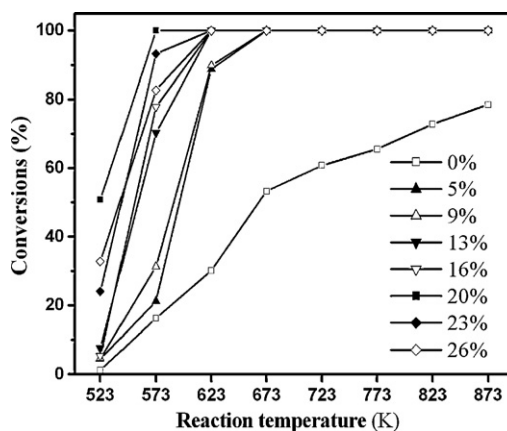


Fig. 6. Acetic acid conversions as a function of temperature for the series of catalysts with different Ni contents. S/C ratio 7.5:1; LHSV = 5.1 h⁻¹; P = 1 atm.

Table 1Influence of the Ni loadings on acetic acid conversions and distribution of the products. $T = 623$ K; S/C ratio 7.5:1; LHSV = 5.1 h^{-1} ; $P = 1$ atm.

Catalysts	C/%	S_{H_2} /%	S_{CH_4} /%	S_{CO} /%	S_{CO_2} /%	$S_{\text{CH}_3\text{COCH}_3}$	$S_{\text{CH}_2\text{CO}}$
La_2O_3	30.1	5.6	6.9	–	46.1	10.4	6.1
5% Ni/ La_2O_3	90.7	87.4	6.2	1.4	81.3	2.4	1.8
9% Ni/ La_2O_3	91.8	88.8	5.1	1.9	83.7	1.7	1.7
13% Ni/ La_2O_3	100	90.7	4.4	1.1	85.5	1.8	1.3
16% Ni/ La_2O_3	100	91.3	3.6	0.8	92.2	0.87	0.78
20% Ni/ La_2O_3	100	93.8	3.4	0.3	94.8	0.38	0.26
23% Ni/ La_2O_3	100	93.2	2.1	1.8	94.6	0.24	0.16
26% Ni/ La_2O_3	100	92.4	2.6	2.9	92.5	0.12	–

reforming reaction. However, the catalytic behaviors were different for the catalysts with different Ni loadings. It could be seen that increasing Ni loadings from 5 to 20 wt.% resulted in a shift of the acetic acid conversion curve toward lower temperatures, besides, the selectivity to H_2 also increased with the increase of Ni loadings, owing to the clear decrease of the formation of CH_4 and the organic by-products, as shown in Table 1. However, further increase the Ni loadings would result in a small but appreciable decrease in catalytic activities, which was more clear at 573 K, where acetic acid conversions increased with the increase of Ni contents and went through the maximum values at 20 wt.% of Ni loadings. Low catalyst loadings might not provide enough sites for the occurrence of the steam reforming. It could be seen that for the catalysts with the lower Ni loadings of 5 and 9 wt.%, acetic acid could not be converted completely until the temperature increasing to 673 K, while for the catalysts with the higher Ni loadings, the temperature at which complete acetic acid conversion was achieved was lowered by more than 50 K. However, it was not the case that the higher Ni loadings, the better performances of the catalyst, because too high Ni loadings would result in some extra Ni crystallites on catalyst surface. The large NiO crystallites in size had no contribution to improve the catalyst activity, vice versa; they would possibly decrease the catalyst activity by forming larger size of Ni particles in the reduction process and then caused the fast metal sintering and coke deposition on catalyst [38]. Therefore, we speculated the 20 wt.% was the optimal metal loadings on La_2O_3 carrier for achieving the best catalytic performances. Therefore, a further research, such as characterizations and influences of reaction temperature, LHSV, S/C and time on stream on the reactions, over this catalyst was conducted.

3.4. Effects of reaction temperature

Typical experimental results showing the catalytic behaviors of Ni/ La_2O_3 catalyst at different temperatures were presented in Fig. 7, in which the conversions of acetic acid and selectivity to each product were shown as a function of reaction temperature that ranged from 523 to 873 K. It could be seen the catalyst showed activity for the reforming reactions even at the initial lower reaction temperature of 523 K, where acetic acid conversion attained about 50%, along with a certain amount H_2 , CO_2 , CO, acetone, ketene and CH_4 as the products. Among them CO was the main gaseous by-product, while acetone and ketene were the main liquid by-products. The substantial amount of CO generation at 573 K might be caused by that the CO adsorbed on catalyst surface could not be removed effectively by the shift reaction [Eq. (5)], owing to the too low reaction temperature.



The production of acetone and ketene implied that besides steam reforming acetic acid the dehydration and bimolecular ketonization of acetic acid also involved as the parallel reactions, which competed with the steam reforming reaction to hydrogen. It might be caused by that the C–C bond of acetic acid molecule

could not be cracked effectively because of the low reaction temperature; consequently, the homogeneous reactions of acetic acid itself proceeded. While as the temperature increasing to 623 K, the desired steam reforming and shift reactions were predominant, acetic acid was then converted completely, and the selectivity to the by-product CO underwent a minimum, decreasing substantially from about 14.1% at 523 K to about 0.24% at 623 K. Meanwhile, the amount of undesired organic by-products acetone and ketene were also presented in trace level. As a result, at 623 K, the selectivities to H_2 and CO_2 passed through the maximum values of 93.8 and 94.8%, respectively. Obviously, Steam reforming of acetic acid could take place to a significant extent over Ni/ La_2O_3 at temperature above 623 K, as evidenced by the sharp increase of catalyst activity and selectivity. However, the selectivity to H_2 did not increase further along with the temperature continuously increasing to higher ranges, for the formation of CO recovered to increase and the amounts increased rapidly with the increase of temperature. Furthermore, the selectivity to CH_4 also started to increase. Clearly, it was unfavorable for hydrogen production at higher temperature because of the two main gaseous by-products, CH_4 and CO.

It is well-known that the production of CH_4 and CO would diminish hydrogen selectivity, 1 mol of CH_4 generation will result in 4 mol loss of H_2 , similarly, 1 mol CO will lose 1 mol of H_2 . Thus, a further research on the pathways of their generations is necessary. the decomposition of acetic acid, we speculated that another possible route for the formation of methane was through methanation of carbon oxides in the steam reforming process, since that Ni had been widely investigated as the active species [39,40] for the methanation of carbon oxides [Eqs. (6) and (7)] and the effluent gas from acetic acid reforming was mainly H_2 and CO_2 . While for CO, the shift reaction itself is exothermic and therefore favored at relatively low temperatures, at high temperatures the reverse shift reaction [Eq. (8)] would be predominant [41], hence we speculated that the reverse shift reaction also occurred in parallel with acetic

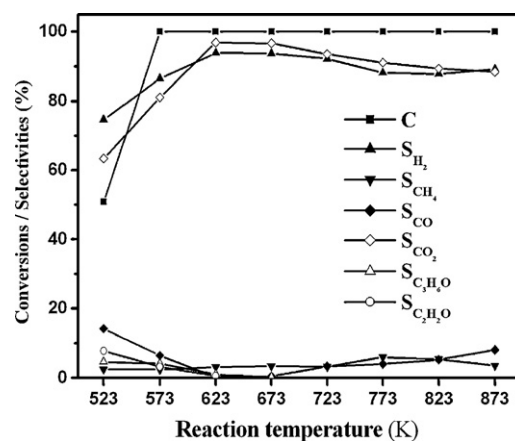


Fig. 7. Effects of reaction temperature on the steam reforming reactions. Catalyst: Ni/ La_2O_3 (20 wt.%); S/C ratio 7.5:1; LHSV = 5.1 h^{-1} ; $P = 1$ atm.

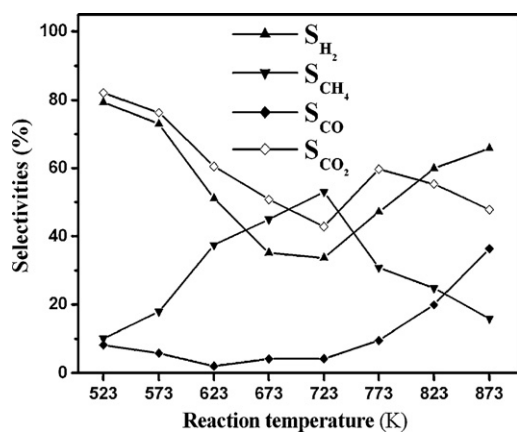
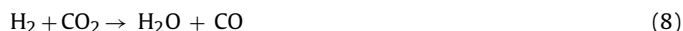


Fig. 8. Distribution of the products in the methanation reactions. The temperature of the first reactor was fixed at 873 K. Catalyst: Ni/La₂O₃ (20 wt.%); GHSV = 2400 h⁻¹; P = 1 atm.

acid steam reforming, especially in higher temperature ranges. To prove the hypothesis, we conducted the methanation reactions over Ni/La₂O₃ catalyst using two reactors in the temperature region of 523–873 K. Acetic acid was firstly reformed with steam in the first reactor to generate the effluent gas, which was then introduced into the second reactor to figure out methanation activity of the catalyst. The distribution of the products obtained from the second reactor as a function of reaction temperature was summarized in Fig. 8. It could be observed that in the lower temperature region of 523–723 K, the selectivity to CH₄ increased rapidly and reached the maximum value of 53.1% at 723 K, leading to the substantial decrease of H₂ and CO₂ selectivities. However, further increasing temperature did not result in the further increase of CH₄ selectivity, owing to the limitations of thermodynamic equilibrium of the reaction. The curve of CH₄ selectivity as a function of reaction temperature in the acetic acid reforming process was shown in Fig. 8, in which CH₄ amounts increased slowly but linearly with the temperature increase from 523 to 773 K and then decreased slightly with the temperature continuously increase. It was approximately in agreement with the results of the methanation experiments, suggesting that in the reforming process the methanation reaction might be one of the pathways for the CH₄ generation, especially at mild temperatures such as 673 K.



Besides, it could be observed an interesting phenomenon. The production of CO exhibited a different characteristic from that of CH₄. It could be observed that the amounts of CO decreased initially but then increased quickly with temperature increase and reached a remarkable level at higher temperature, as shown in Fig. 8. Evidently, the methanation of CO took place at the lower temperature of 523 K, the formation of CO then decreased and underwent a minimum at 623 K, which was well in accordance with the results shown in Fig. 7. Therefore, we concluded that the shift reaction and the methanation of CO were the two main reasons for the sharp decrease of CO formation at 623 K in the reforming process. While along with the temperature continuously increase, the rate of the reverse shift reaction accelerated and exceeded that of CO methanation, as a consequence, CO amounts recovered to increase and reached a remarkable level in higher temperature ranges. Summarized the above results, we concluded that CO concentration was governed by the shift and methanation reactions in the lower temperature ranges in the reforming process, while in

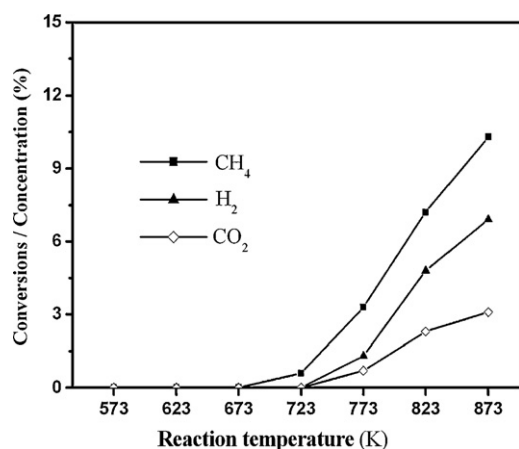


Fig. 9. The steam reforming of methane. Catalyst: Ni/La₂O₃ (20 wt.%); S/C ratio 5:1; GHSV = 8400 h⁻¹; P = 1 atm.

higher temperature ranges it was mainly governed by the reverse shift reaction.

In addition to the methanation and reverse shift reactions in the reforming reactions, we speculated the steam reforming of CH₄ [Eqs. (9) and (10)] also might have some impact on the distribution of the products at higher temperatures, since steam was excess in the reactants and the Ni-based catalysts were effective for CH₄ reforming [42].



Besides, the steam reforming CH₄ also could explain the decrease in the formation of CH₄ and increase of CO amounts at higher temperature. Therefore, in order to examine this possibility, additional experiments of steam reforming CH₄ were conducted over Ni/La₂O₃ catalyst under the similar reaction conditions of acetic acid reforming. Results were shown in Fig. 9. It could be seen that at the temperature below 773 K, the catalyst showed negligible activity. While at the maximum reaction temperature of 873 K, the catalyst still showed very poor activity to convert CH₄. Only a small amount of H₂ and CO₂ generated and no CO formation were observed, indicating that the steam reforming of CH₄ had an insignificant influence on the distribution of the products in the reforming process. To summarize, in higher temperature region, the methanation reaction was the important pathways for CH₄ generation, while the reverse shift reaction was responsible for the appreciable amount of CO formation.

3.5. Effects of LHSV

The effects of LHSV on the catalytic performances of Ni/La₂O₃ catalyst were investigated at 573 and 623 K, respectively. Results were illustrated in Figs. 10 and 11. It could be observed the distinct effects of LHSV on the reforming reactions under the different reaction temperature. At lower temperature of 573 K, increasing the LHSV resulted in the sharp decrease of acetic acid conversions, together with a significant decrease in H₂ and CO₂ production. While as regard the by-products, the case was complicated. A mild decrease in CH₄ selectivity was observed, however, along with the increase of LHSV, the selectivity to other by-products such as CO, acetone and ketene all increased remarkably, especially the CO selectivity, which increased progressively from less than 5% at 3.3 h⁻¹ to about 30% at 12.3 h⁻¹. We speculated the low conversions of acetic acid might be caused by the limited specific area of the catalyst and the low steam reforming rates at the low reaction temperature. While at higher space velocity the lower contact

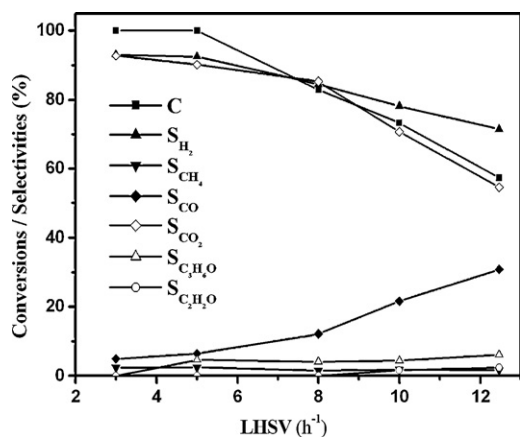


Fig. 10. Influence of LHSV on the conversions of acetic acid and selectivities to the products at 573 K. Catalyst: Ni/La₂O₃ (20 wt.%); $T=573$ K; S/C ratio 7.5:1; $P=1$ atm.

time was unfavorable for the adsorption and activation of steam and acetic acid, as a result, the steam reforming and shift reactions could not work sufficiently and then the ketonization and dehydration reactions proceeded, leading to the large amount of CO, acetone and ketene generation. As for CH₄, we considered a part of it come from the methanation of carbon oxides. When higher LHSV was imposed, the limited catalyst surface was mainly adsorbed by the molecules of acetic acid and steam. Consequently, the H₂ and carbon oxides might have less chance to contact with catalyst active sites to form CH₄, thus, it was the results that the higher LHSV, the lower selectivity to CH₄. However, increasing temperature by 50 K could result in a remarkable improvement of the catalytic activity and selectivity. As shown in Fig. 11. Acetic acid conversion kept 100% for the whole range of LHSV investigated. Although the selectivities to H₂ and CO₂ still decreased at higher space velocity, they did not drop so dramatically as that of 573 K. There still was a significant amount of CO formed at higher space velocity, but the amount was in trace level at lower space velocity, and selectivities to other by-products were all decreased with the increase of LHSV. Apparently, at 623 K, the catalyst showed relatively better tolerance space velocity, since the steam reforming rates accelerated and the reactants could be activated enough to form H₂ and diminish the by-products generation.

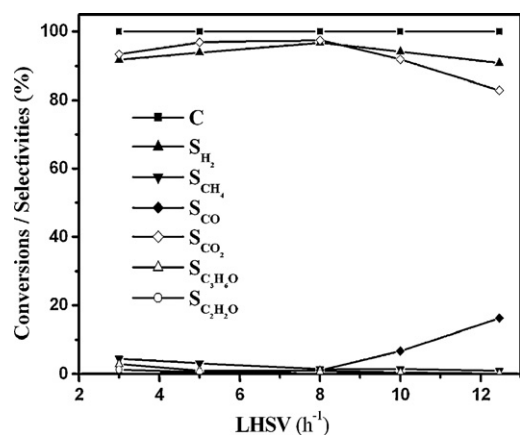


Fig. 11. Influence of LHSV on the conversions of acetic acid and selectivities to the products at 623 K. Catalyst: Ni/La₂O₃ (20 wt.%); $T=623$ K; S/C ratio 7.5:1; $P=1$ atm.

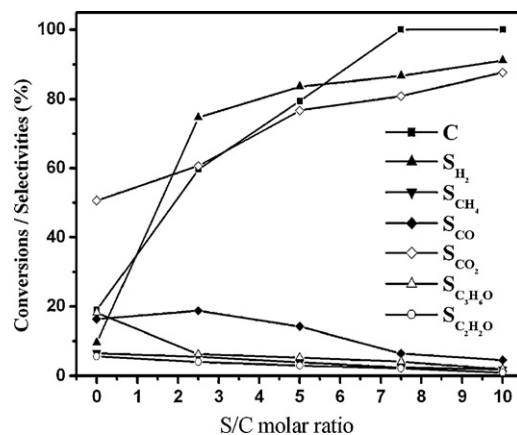


Fig. 12. Effects of S/C on the conversions of acetic acid and distribution of the products at 573 K. Catalyst: Ni/La₂O₃ (20 wt.%); $T=573$ K; LHSV = 5.1 h⁻¹; $P=1$ atm.

3.6. Effects of S/C

S/C was one of the key parameters in the reforming reactions, influences of which on the steam reforming reaction were also investigated at 573 and 623 K, respectively. Results were given in Figs. 12 and 13, where acetic acid conversions and distribution of the products were plotted as functions of the S/C ratios that ranged from 0 to 10:1. It could be seen that whether acetic acid conversions or selectivities to H₂ and CO₂ all increased monotonously with the increase of S/C ratios, conversely, the formation of the by-products decreased at high S/C ratios. Clearly, excess steam could favor the steam reforming reactions and depress the generation of the by-products. Marquovich et al. also reported low S/C ratios would result in low rate of the steam reforming and large amount by-products generation, owing to the low partial pressure of steam [8]. Moreover, it could be seen in the absence of steam, that is, at the S/C ratio of 0, the acetic acid ketonization, dehydration and decomposition reactions were dominant, resulting in almost no H₂ formation. While in the presence of steam, these reactions were depressed to a significant extent. Such as at the S/C ratio of 2.5:1, the steam reforming of acetic acid proceeded, acetic acid conversion and H₂ yield increased substantially. However, the selectivity to H₂ was still relatively low because of the significant amount of CO generation. It might be caused by that CO was more difficult to be removed by the shift reaction at low steam ratios, which was proved by the subsequent runs conducted at higher S/C ratios, CO selectivity decreased linearly along with the increase of S/C ratios. Obviously, at high steam ratios, not only the shift reaction was

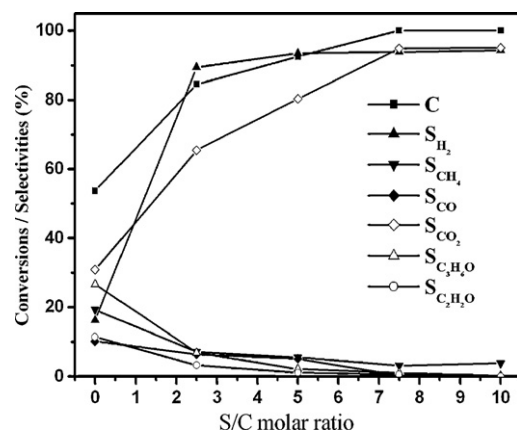


Fig. 13. Effects of S/C on the conversions of acetic acid and distribution of the products at 623 K. Catalyst: Ni/La₂O₃ (20 wt.%); $T=623$ K; LHSV = 5.1 h⁻¹; $P=1$ atm.

promoted but also the reverse shift reaction was inhibited to some extent. Higher temperature could result in higher steam reforming rates and better activation of the reactants, and then better catalytic performances were obtained, as the results shown in Fig. 13. At 623 K, the catalytic activity and selectivity were improved remarkably. At the same S/C ratios, higher acetic acid conversions and H₂ yields were achieved. Moreover, the formation of the by-products were all suppressed to a significant extent, especially for CO, at the S/C ratios above 7.5:1, it was only detected in trace amount.

At 573 K, there were pronounced amounts of CO and CH₄ generation and the amounts increased substantially along with the decrease of S/C ratios. Hence, it was worthy to discuss the influences of S/C ratios on the by-products generation here at this low reaction temperature. In Section 3.4, we had elucidated that in higher temperature ranges part of CO and CH₄ were the secondary products, the methanation and reverse shift reactions were the important pathways for their generations. However, at lower reaction temperature such as 573 K, it seemed not to be the case, especially for CO. It was well established in the literature that the reverse shift reaction was favored at higher temperature, in lower temperature region, the shift reaction was dominant [41]. Apparently, the reverse shift reaction could not explain the significant amount of CO formation at the temperature below 623 K. CO might be the primary products that come directly from the steam reforming acetic acid. As for CH₄, we thought another route that CH₄ was formed directly by the decomposition of acetic acid [Eq. (3)] might work at lower S/C ratios, for the catalyst showed relatively lower activity for the methanation reaction at temperature below 623 K and the decomposition of acetic acid was favored at lower steam ratios.

Wang et al. reported that acetic acid was dissociative adsorption to form CO_x, CH_x and H_{ads} species on catalyst surface in the steam reforming process [10]. Low S/C ratios meant less proportion of steam in the reactants, which would inevitably affect the adsorption of steam and then result in less OH_{ads} species formed by the dissociation of steam. Consequently, the CH_x species would have more chance to combine with H_{ads} species, and then desorbed to form the by-product CH₄, or combined with only one OH_{ads} species and then dehydrogenated to form CO_{ads} species. However, the CO_{ads} species was difficult to be removed by the shift reaction at lower S/C ratios due to the less OH_{ads} species formed on catalyst surface, consequently, another by-product CO formed. Therefore, we thought that low S/C would affect the adsorption of steam and then the shift reaction, which, as a result, lead to the lower conversions of acetic acid and higher selectivities to CO and CH₄. Besides, Markevich et al. pointed out that the organic and steam competed in metal sites in the reforming process, S/C would have remarkable influence on catalytic activity and selectivity if the active sites on catalyst surface were limited [43]. The characterization showed that Ni/La₂O₃ catalyst had limited specific area, which might result in the competing for active sites between acetic acid and steam, and then influenced the distribution of the products, as the results presented above.

3.7. Stability test

Taking into account that Ni/La₂O₃ catalyst showed the best performances at 623 K, stability test was carried out at this temperature to better insight into its catalytic behaviors. The test performed for 100 h, results were shown in Fig. 14, in which acetic acid conversions, and selectivities to the products were plotted as functions of time. It could be seen that Ni/La₂O₃ catalyst exhibited the stable performances for the 100 h investigated, showing no deactivation signs. Conversions of acetic acid kept the practically constant values of 100% for all the time-on-stream, while distribution of the products varied with the prolonged reaction time. It was noteworthy that the formation of the highly undesirable

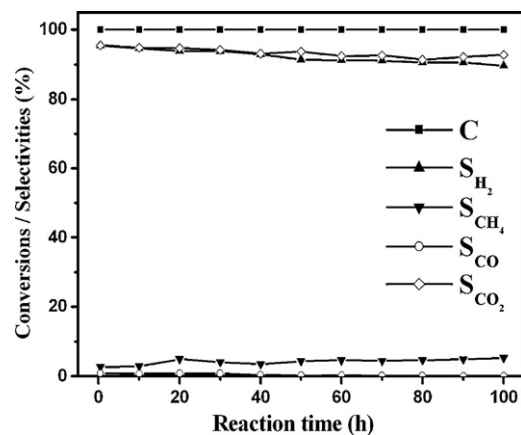


Fig. 14. Stability test. Catalyst: Ni/La₂O₃ (20 wt.%). T = 623 K; S/C ratio: 7.5:1; LHSV = 5.1 h⁻¹; P = 1 atm.

by-product CO decreased with the reaction time and after 40 h in the effluent gas, its presence in the effluent gas was in trace amount, which was of significance for the use of acetic acid as the promising fuel for PEMFC. Besides, there was negligible amount of acetone generation at the initial reaction time, but it could not be detected anymore after several hours of time-on-stream, thus, we did not express it in Fig. 14. However, the amount of another main by-product CH₄ increased remarkably after 20 h but then stabilized after 50 h. Consequently, the selectivities to H₂ and CO₂ dropped correspondingly, but the values still exceeded 90%, and further exposure of the catalyst to the reactants mixture did not result in the further decrease of the selectivities. The stable internal structure of Ni/La₂O₃ catalyst might be one of the reasons for its good performances in the stability test. Liang et al. reported that the rare earth oxide, La₂O₃, could prevent Ni metal from agglomerating by supporting and isolating the particles, and then promoted Ni dispersion and restricted the increase of the particle size [44]. From the XRD results, we also could observe that there was no remarkable increase of Ni particle size in spent catalyst, which is very advantageous for the steam reforming reactions. While Fleys et al. also reported that nickel particles could be dispersed in the lanthanum oxide matrix and formed an overlayer that contained both lanthanum and nickel which could explain the stable and active performances of the catalyst [37].

There are some reports [45–47] that hydrocarbons are easily polymerized and form coke on metal sites, which will make the catalyst lose activity. However, of special interest is the uniqueness of the Ni/La₂O₃ in terms of its long term stability and good resistibility to carbon deposition, which also has been observed for reforming of CH₄ with CO₂ [48]. Fatsikostas et al. have explained this phenomenon by taking into account a mechanistic model that a thin overlayer of lanthana is formed on top of the nickel particles during their work of steam reforming of ethanol [49]. Under the reforming reaction conditions, lanthanum oxides species, which decorated the Ni particles, reacted with CO₂ to form La₂O₂CO₃ [Eq. (11)]. The lanthanum oxycarbonate species then reacted with surface carbon, at their periphery, thus cleaning the carbon deposits on Ni surface [Eq. (12)].



In this way, the surface carbon at the periphery of the oxycarbonate particles was removed, leading to the observed good stability of the catalyst. There is also a body of other work on the beneficial effect of lanthanide oxides in the stability of Ni-based catalysts since these oxides are known promoters of carbon removal

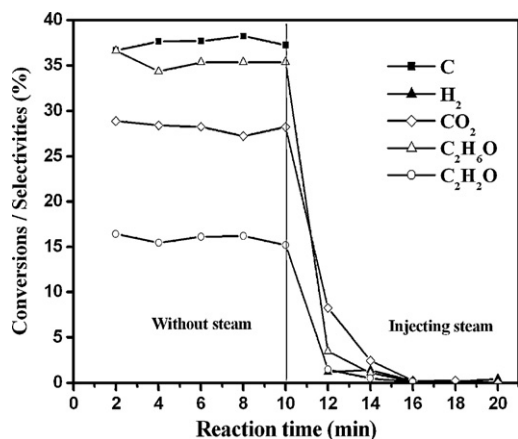


Fig. 15. Acetic acid pulse experiments in the absence and presence of steam over La_2O_3 . Catalyst: La_2O_3 . $T = 623 \text{ K}$; $\text{LHSV} = 5.1 \text{ h}^{-1}$; $P = 1 \text{ atm}$.

from metallic surfaces [50,51]. Besides, the steam reforming reaction was conducted at a high steam to carbon ratio, the excess steam also was a very effective factor to resist carbon deposition, which could gasify [Eq. (13)] and then eliminated the surface carbon on catalyst.



The carbon balance calculated from carbon products was higher than 97% throughout the stability test. Moreover, from the XPS results of the spent catalyst, although we observed the carbon concentration increase on the surface of the catalyst, the increase was very little and negligible, suggesting that the carbon deposition rate was relatively low under the experimental conditions employed, the catalyst showed good resistibility to carbon deposition.

3.8. Roles of Ni and La_2O_3 in the steam reforming reaction

It was recognized that the steam reforming process involved the important steps of the adsorption and activation of acetic acid. To make sure where acetic acid was activated, we conducted the pulse experiments over La_2O_3 and $\text{Ni/La}_2\text{O}_3$, respectively. The experiments were carried out by introducing pure acetic acid into the reactor for 10 min to make sure catalyst surface was adsorbed sufficiently, then the pulse of acetic acid was stopped and steam was introduced into the reactor for another 10 min to gasify the adsorbed species. The products were detected on-line by the chromatograms. It could be seen from Fig. 15 that acetone and ketene was the main by-products over La_2O_3 in the absence of steam, which mainly came from the homogeneous reactions. When acetic acid pulse was stopped and steam introduced, there was no H_2 formation, and the organic products and CO_2 productions declined very quickly along with time, indicating that acetic acid could not be dissociably adsorbed on La_2O_3 surface to form the methyl, CO_x and other species that were the important intermediate for the proceeding of the steam reforming process. In Section 3.3, we also had shown that over La_2O_3 there was almost no hydrogen formation, the support itself showed no steam reforming activity, probably due to its poor capacity of activating acetic acid. While for $\text{Ni/La}_2\text{O}_3$ catalyst, the case was different. As shown in Fig. 16. The catalyst showed remarkably high activity for converting acetic acid, and there was some H_2 generation, which mainly came from acetic acid decomposition. More importantly, when steam was introduced into the reactor, the yields of typical steam reforming products such as H_2 , CO_2 , CO and CH_4 , increased substantially. It was clear that metal Ni was the active sites for the reforming reaction. Acetic acid was adsorbed and dissociated over it to form the methyl and

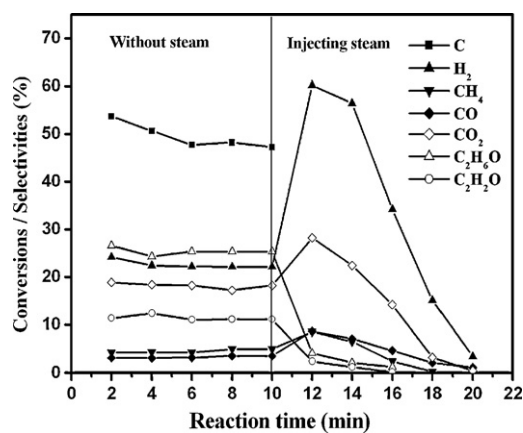


Fig. 16. Acetic acid pulse experiments in the absence and presence of steam over $\text{Ni/La}_2\text{O}_3$ (20 wt.%). Catalyst: $\text{Ni/La}_2\text{O}_3$ (20 wt.%). $T = 623 \text{ K}$; $\text{LHSV} = 5.1 \text{ h}^{-1}$; $P = 1 \text{ atm}$.

CO_x species, which then reacted with steam to form H_2 . Although La_2O_3 had poor activity of activating acetic acid, it was an important medium for the activation of steam. It was reported that steam could be adsorbed on La_2O_3 surface and then mobilized to metal sites to participate in the steam reforming reaction [30]. Besides, as discussed in Section 3.7, La_2O_3 was one of the important factors for the elimination of the carbon deposits on catalyst surface.

3.9. Reaction pathways

Based on the results outlined above, we suggested a schematic representation of reaction pathways involved in the formation of H_2 , CO_2 , CO , CH_4 , acetone and ketene from acetic acid steam reforming over $\text{Ni/La}_2\text{O}_3$ catalyst. As illustrated in Figs. 17 and 18. The dissociation pattern of acetic acid and the pathways for the formation of acetone and ketene was shown in Fig. 17. Here the * represented the metal sites. There were mainly two ways for the dissociation of acetic acid, cleavage the H–O and C–O bonds formed the acetate and acyl species, respectively [52]. Here the acetate species would undergo further decompose to form adsorbed methyl and CO_2 , similarly, the acyl species could decompose to form methyl and CO^* , but it also could integrate with the methyl group to form acetone. It could be observed here that whether acetic acid dissociated to acetate species or acyl species, further decomposition of them all gave methyl species, which was an important intermediate in the steam reforming process, it was the precursors for the formation of gaseous products, as shown in Fig. 18. The methyl group could combine with one *OH species and then dehydrogenated to form H_2 and CO^* , the CO^* was then removed by the shift reaction. It also could further dehydrogenate to form CH_2^* and then combined with two *OH species, which then gave the products of H_2 and CO_2 . In addition, the methyl also could combine with *H to form the by-product CH_4 , or further decompose to form C^* species, which would accumulate and block the surface sites and then decreased catalyst activity. Nevertheless, under the experimental conditions employed, most of the C^* formed could be gasified by steam and CO_2 . Besides, the dissociation of steam and the recombination of two H^* species to form H_2 also were important steps involved in the steam reforming process. From Fig. 18, we could find another intermediate that was very important for the formation H_2 in the steam reforming process was *OH species, it could integrate with CH_x ($x = 0-3$) to form the gaseous carbon products and, most importantly, to form H_2 . Furthermore, *OH was also an important species to suppress the by-products generation. It could not only prevent the further dissociation of methyl to carbon deposits and the combination of methyl group with *H to

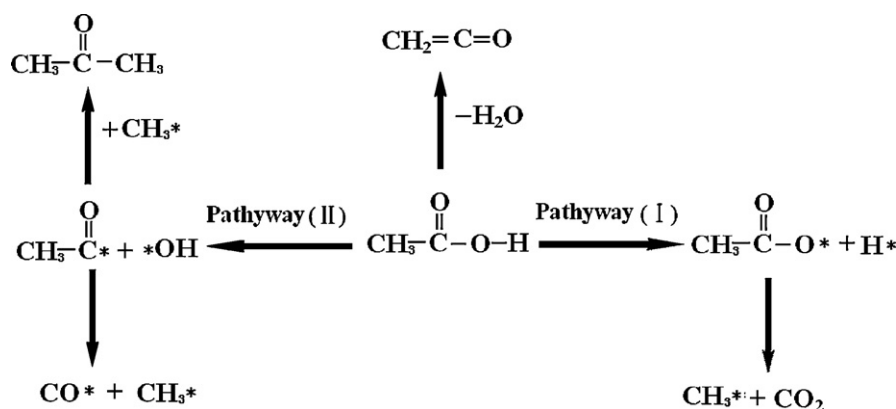


Fig. 17. The dissociation patterns of acetic acid on catalyst surface.

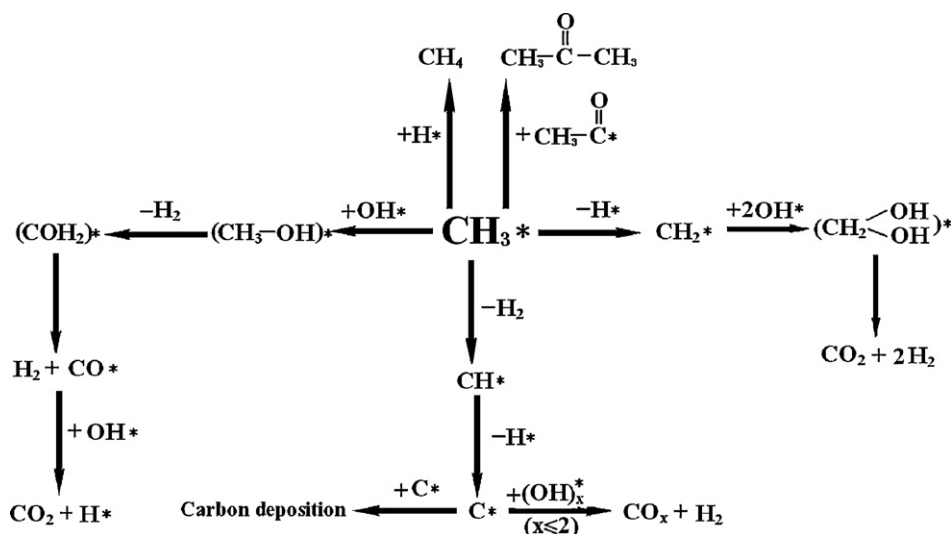


Fig. 18. Assumed reaction pathways involved in the steam reforming process.

CH_4 , but also could eliminate CO generation through the shift reaction.

4. Conclusion

To sum up, the present results demonstrated that the novel Ni/La₂O₃ catalyst could produce hydrogen via acetic acid steam reforming at relatively mild temperature effectively. At the Ni loading of 20 wt.%, the catalyst exhibited the best catalytic performances. The characterizations showed there were strong interactions between Ni and La species. Ni was the active sites for the proceeding of the reforming reactions. While La₂O₃ itself had no contribution for the activation of acetic acid, but it could effectively adsorb steam and react with CO₂ to form La₂O₂CO₃, which could further react with the surface carbon deposits and then restore the catalyst activity.

In the steam reforming reactions, acetone and ketene was the main organic by-products at the temperature lower than 673 K, they mainly come from bimolecular ketonization reaction and acetic acid dehydration, respectively. While CH₄ and CO was the main gaseous by-products in the effluent gas, the decomposition of acetic acid and the methanation of carbon oxides were the two main pathways for CH₄ generation; as for the production of CO, the amount was mainly governed by the shift and the reverse shift reactions. According to the experimental results, we speculated that methyl species was the important intermediate

in the reforming process, it could form CH₄, CO, CO₂ and acetone through the combination with H*, *OH or acyl species, respectively, while *OH was another important intermediate that was important for the formation of H₂ and elimination of the by-products generation.

At lower reaction temperature 573 K, space velocity and S/C had remarkable influence on the conversion of acetic acid and distribution of the products, particularly at higher space velocity and lower S/C, acetic acid conversion was very low and a significant amount of by-products were produced. However, increasing the reaction temperature and the S/C ratios could remarkably improve the catalytic activity and selectivity, since lower reaction temperature and S/C resulted in lower steam reforming rates. At a selected experimental condition of $T=623\text{ K}$, $\text{LHSV}=5.1\text{ h}^{-1}$ and $\text{S/C}=7.5:1$, the catalyst showed high activity, selectivity and, most importantly, good long-term stability for hydrogen production. Therefore, we thought Ni/La₂O₃ was a promising catalyst, which made the steam reforming acetic acid become feasible and open an opportunity to the use of a new renewable energy source for hydrogen production.

Acknowledgements

We acknowledge the financial support of the 973 Project of China (G2003CB214503). We are grateful to Qunyang Gao and Xiaojie Zhang for their help in the characterizations of the catalyst.

References

- [1] H.J. Eom, J.H. Janga, D.W. Leeb, S. Kima, K.Y. Lee, J. Mol. Catal. A: Chem. 349 (2011) 48.
- [2] H. Song, U.S. Ozkan, J. Mol. Catal. A: Chem. 318 (2010) 21.
- [3] L.Z. Zhang, X.Q. Wang, B. Tan, U.S. Ozkan, J. Mol. Catal. A: Chem. 297 (2009) 26.
- [4] X. Hu, C.-Z. Li, Green Chem. 13 (2011) 1676.
- [5] X. Hu, C. Lievens, A. Larcher, C.-Z. Li, Bioresour. Technol. 102 (2011) 10104.
- [6] Y. Matsumura, H. Ishibe, J. Mol. Catal. A: Chem. 345 (2011) 44.
- [7] T. Milne, F. Agblevor, M. Davis, S. Deutch, D. Johnson, in: A.V. Bridgwater, D.G.B. Boocock (Eds.), *Developments in Thermochemical Biomass Conversion*, Blackie, London, 1997, pp. 409–424.
- [8] M. Markevich, S. Czernik, E. Chornet, D. Montane, Energy Fuels 13 (1999) 1160.
- [9] D. Wang, S. Czernik, D. Montane, M. Mann, E. Chornet, Ind. Eng. Chem. Res. 36 (1997) 1507.
- [10] D. Wang, D. Montane, E. Chornet, Appl. Catal. A: Gen. 143 (1996) 245.
- [11] J.R. Galdamez, L. Garcia, R. Bilbao, Energy Fuels 19 (2005) 1133.
- [12] F. Bimbela, M. Oliva, J. Ruiz, L. García, J. Arauzo, J. Anal. Appl. Pyrolysis 79 (2007) 112.
- [13] K. Takanabe, K. Aika, K. Seshan, L. Lefferts, J. Catal. 227 (2004) 101.
- [14] K. Takanabe, K. Aika, K. Inazu, T. Baba, K. Seshan, L. Lefferts, J. Catal. 243 (2006) 263.
- [15] K. Takanabe, K. Aika, K. Seshan, L. Lefferts, Chem. Eng. J. 120 (2006) 133.
- [16] C. Rioche, S. Kulkarni, F.C. Meunier, J.P. Breen, R. Burch, Appl. Catal. B: Environ. 61 (2005) 130.
- [17] X. Hu, G. Lu, Chem. Lett. 35 (2006) 452.
- [18] X. Hu, G. Lu, J. Mol. Catal. A: Chem. 261 (2007) 43.
- [19] J.H. Sinfelt, Adv. Catal. 23 (1973) 91.
- [20] C. Oliva, C. Berg, J.W. Niemantsverdriet, D. Curulla-Ferre, J. Catal. 245 (2007) 436.
- [21] E. Heracleous, A.F. Lee, K. Wilson, A.A. Lemonidou, J. Catal. 231 (2005) 159.
- [22] J. Xi, Z. Wang, G. Lu, Appl. Catal. A: Gen. 225 (2002) 77.
- [23] H.V. Fajardo, L.F.D. Probst, Appl. Catal. A: Gen. 306 (2006) 134.
- [24] J. Kugai, V. Subramani, C. Song, M.H. Engelhard, Y. Chin, J. Catal. 238 (2006) 430.
- [25] G. Mul, A.S. Hirschon, Catal. Today 65 (2001) 69.
- [26] J. Petryk, E. Kowakowska, Appl. Catal. B: Environ. 24 (2000) 121.
- [27] S. Irusta, L. Cornaglia, E. Lombardo, J. Catal. 210 (2002) 263.
- [28] H. Vidal, S. Bernal, R. Baker, G. Cifredo, D. Finol, J. Rodriguez-Izquierdo, Appl. Catal. A: Gen. 208 (2001) 111.
- [29] S. Kus, M. Otremba, M. Taniewski, Fuel 82 (2003) 1331.
- [30] T.J. Toops, A.B. Walters, M.A. Vannice, Appl. Catal. B: Environ. 38 (2002) 183.
- [31] M.C. Sanchez-Sanchez, R.M. Navarro, J.L.G. Fierro, Int. J. Hydrogen Energy 32 (2007) 1462.
- [32] A.N. Fatsikostas, X.E. Verykios, J. Catal. 225 (2004) 439.
- [33] J. Sun, X.P. Qiu, F. Wu, W.T. Zhu, Int. J. Hydrogen Energy 30 (2005) 437.
- [34] X.H. Yu, S.C. Zhang, L.Q. Wang, Q. Jiang, S.G. Li, Z. Tao, Fuel 85 (2006) 1708.
- [35] X. Hu, G. Lu, Catal. Commun. 12 (2010) 50.
- [36] Z. Xu, Y. Li, J. Zhang, L. Chang, R. Zhou, Z. Duan, Appl. Catal. A: Gen. 210 (2001) 45.
- [37] M. Fleys, Y. Simon, D. Swierczynski, A. Kiennemann, P. Marquaire, Energy Fuels 20 (2006) 2321.
- [38] A. Teixeira, R. Giudici, Chem. Eng. Sci. 54 (1999) 3609.
- [39] X. Hu, G. Lu, Appl. Catal. B: Environ. 99 (2010) 289.
- [40] X. Hu, G. Lu, Int. J. Hydrogen Energy 35 (2010) 7169.
- [41] S. Specchia, F.W.A. Tillemans, P.F.V. Oosterkamp, G. Saracco, J. Power Sources 145 (2005) 683.
- [42] T. Nozaki, N. Muto, S. Kado, K. Okazaki, Catal. Today 89 (2004) 57.
- [43] M. Markevich, F. Medina, D. Montane, Catal. Commun. 2 (2001) 119.
- [44] Q. Liang, L.Z. Gao, Q. Li, S.H. Tang, B.C. Liu, Z.L. Yu, Carbon 39 (2001) 897.
- [45] X. Hu, G. Lu, Green Chem. 11 (2009) 724.
- [46] D.L. Trimm, Catal. Today 37 (1997) 233.
- [47] X. Hu, G. Lu, Energy Fuels 23 (2009) 926.
- [48] Z.L. Zhang, X.E. Verykios, J. Chem. Soc. Chem. Commun. 1 (1995) 71.
- [49] A.N. Fatsikostas, D.I. Kondarides, X.E. Verykios, Catal. Today 75 (2002) 145.
- [50] D. Srinivas, C.V.V. Satyanarayana, H.S. Potdar, P. Ratnasamy, Appl. Catal. A: Gen. 246 (2003) 323.
- [51] A.N. Fatsikostas, D.I. Kondarides, X.E. Verykios, Chem. Commun. 9 (2001) 851.
- [52] K.I. Gursahani, R. Alcalá, R.D. Cortright, J.A. Dumesic, Appl. Catal. A: Gen. 222 (2001) 369.